Materials Science Forum
ISSN: 1662-9752, Vol. 1062, pp 235-240
doi:10.4028/p-621n11
© 2022 The Author(s). Published by Trans Tech Publications Ltd, Switzerland.
Submitted: 2022-01-26
Accepted: 2022-02-25
Online: 2022-05-31

# Mechanism Governing Surface Roughening of Al Ion Implanted 4H-SiC during Annealing under a C-Cap

Mariaconcetta Canino[1,a*], Fulvio Mancarella[1,b], Filippo Bonafè[1,c], Franco Corticelli[1,d], Cristiano Albonetti[2,e], and Roberta Nipoti[1,f]

[1]CNR-IMM of Bologna, via Gobetti 101, 40129 Bologna, Italy

[2]CNR-ISMN of Bologna, via Gobetti 101, 40129 Bologna, Italy

[a]canino@bo.imm.cnr.it, [b]mancarella@bo.imm.cnr.it, [c]bonafe@bo.imm.cnr.it, [d]corticelli@bo.imm.cnr.it, [e]cristiano.albonetti@cnr.it, [f]nipoti@bo.imm.cnr.it

**Keywords:** 4H-SiC, ion implantation, annealing, roughness

**Abstract.** Encapsulating SiC with a carbon layer (C-cap) is a widely used technique to avoid step bunching during post implantation annealing. In this work we propose a mechanism that explains the roughening that the surface unavoidably undergoes during annealing under the C-cap. We investigated the reactions occurring at the interface between 4H-SiC and the C-cap by scanning electron microscopy, energy-dispersive X-ray spectroscopy, and atomic force microscopy carried out at different stages of the sample processing: just after annealing, after C-cap removal in dry Oxygen, and after cleaning in buffered oxide etch solution. Our observations show that, even though the C-cap roughens for increasing annealing temperature and time, it is not visibly damaged even after 1950 °C 30 min annealing. After the C-cap removal the 4H-SiC surface was covered by a network of clusters that are eventually removed by buffered oxide etch solution. This occurrence suggests that, during the post-implantation annealing, the 4H-SiC surface decomposes and the escaped Si and C atoms are trapped inside the C-cap or at the interface between 4H-SiC and the C-cap. While C clusters are etched off in the dry $O_2$ atmosphere, the Si clusters oxidize and form $SiO_2$ nanoparticles which are finally etched by buffered oxide etch.

## Introduction

The electrical activation of Al in 4H-SiC is often carried out at annealing temperatures exceeding 1650 °C [1]. At such elevated temperatures, two detrimental occurrences are observed: step bunching of the SiC surface and increasing of the concentration of carbon vacancies [2], a lifetime killer defect for 4H-SiC bipolar devices, in the drift layer. Encapsulating the SiC surface with a carbon layer (C-cap) during post implantation annealing can be beneficial both as a source of carbon atoms, provided that the cooling rate is low enough to maintain carbon vacancy thermal equilibrium [3], and to reduce surface roughening. However, surface changes are not completely prevented. It was observed by several authors that the surface of Al ion implanted 4H-SiC, annealed at temperatures higher than 1750 °C, is featured by holes and the root means square of the surface roughness (rms) is higher than 1 nm [4,5]. It was observed that, for equal annealing treatments, rms increases for increasing Al concentration, and that prolonged annealing, even at temperatures as low as 1650 °C, also results in increased rms [6]. Some authors attribute surface roughening under the C-cap to a deterioration of the C-cap itself [4]. However, the occurrence of material evaporation even under a stable C-cap is not completely ruled out. Indeed, SIMS analyses revealed surface erosion of 4H-SiC subsequent to annealing at 1900 °C and 2000 °C, with durations between 15 min and 1 h, while the surface remained smooth [7]. According to this study, material loss is linked to the lattice damage rather than directly to the Al concentration. In this work, we investigate the changes occurring in the C-cap and at the interface between the C-cap and Al ion implanted 4H-SiC upon annealing at different temperatures and times, at different stages of the sample processing. We find that the C-cap is compact and that, after C-cap removal, the surface is covered by a network of grains, which can be removed by a Buffered Oxide Etch (BOE) solution. A mechanism involving Si and C evaporation from the surface, and trapping inside or below the C-cap is proposed.

This article is an open access article under the terms and conditions of the Creative Commons Attribution (CC BY) license
(https://creativecommons.org/licenses/by/4.0)

## Experimental

Two commercial 4° off-axis (0001) n-type 4H-SiC homo-epitaxial wafers were used. The wafer major flat was parallel to the (1-100) plane with the flat face parallel to the <11-20> direction. Al depth profiles with uniform concentration of $1.0 \times 10^{19}$ cm$^{-3}$ and $1.0 \times 10^{20}$ cm$^{-3}$ extending 200 nm in depth from the wafer surface were created by Al ion implantation at 500 °C. The implanted SiC wafers were diced in piece before post implantation annealing. The C-cap was a layer of OiR908-35 photoresist from Fujifilm spun at 4000 rpm pyrolysed at 900 °C. The annealing was carried out in a RF heated graphite crucible at temperatures between 1750 °C and 1950 °C flowing Ar at 1 atm. The annealing temperature was attained with 1.67 °C/s heating and 0.5 °C/s cooling rates. The C-cap was removed by dry oxidation at 850 °C for 15 min and the 4H-SiC surface was cleaned in buffered oxide etch (BOE) 7:1 for 20 min.

Characterizations were carried out at different stages of sample production. Cleaved cross sections of the samples were observed by a ZEISS Crossbeam 340 BIB/EBL in SEM mode. Energy-dispersive X-ray (EDX) spectroscopy microanalyses on flat surfaces were carried out in a ZEISS EVO|LS10 SEM with a X-Flash 6|30 SDD at 5 kV and 9 11 kpcts. The surface morphology was analysed by a Thermomicroscope Autoprobe CP Research Atomic Force Microscope (AFM) with the fast scan direction parallel to <11-20>.

Table 1 reports processing conditions, rms of the C-cap after annealing and of the 4H-SiC surface after BOE, and the Figures displaying images of each sample. Considered the slow rate of surface evolution occurring at 1700 °C [6], the samples annealed for 15 min and 30 min are considered equal.

**Table 1.** Processing conditions (Al concentration, annealing temperature and time), rms of the annealed C-cap, rms of the 4H-SiC surface after BOE, and Figure numbers showing images of each sample.

| Al [cm$^{-3}$] | T [°C] | Time [min] | rms C-cap [nm] | rms SiC [nm] | Figure |
|---|---|---|---|---|---|
| $1\times10^{20}$ | 1750 | 15 | 1.3 ± 0.3 | | 4(a) |
| $1\times10^{20}$ | 1750 | 30 | | 1.6 ± 0.4 | 4(d) |
| $1\times10^{20}$ | 1850 | 120 | 9.4 ± 0.8 | 8.8 ± 0.2 | 4(b,e) |
| $1\times10^{19}$ | 1950 | 30 | 20 ± 2 | 8.3 ± 0.5 | 1(a-b), 2(a-c), 3(b-d) 4(c,f) |

## Results and Discussion

Figs. 1(a,b) show the C-cap after annealing at 1950 °C for 30 min. The SEM cross section view in Fig. 1(a) shows that the C-cap is (550±20) nm thick, uniformly distributed over the surface, with grains 100-200 nm in size and no pass-through hole. The observation of the cleaved profile reveals that the shape of cleaved C-cap does not reproduce the SiC border, thus leaving the SiC surface partly uncovered. Fig. 1(b) shows the AFM micrograph of the C-cap surface in the center of the sample. The granular structure of the C-cap surface is confirmed by the AFM analyses.

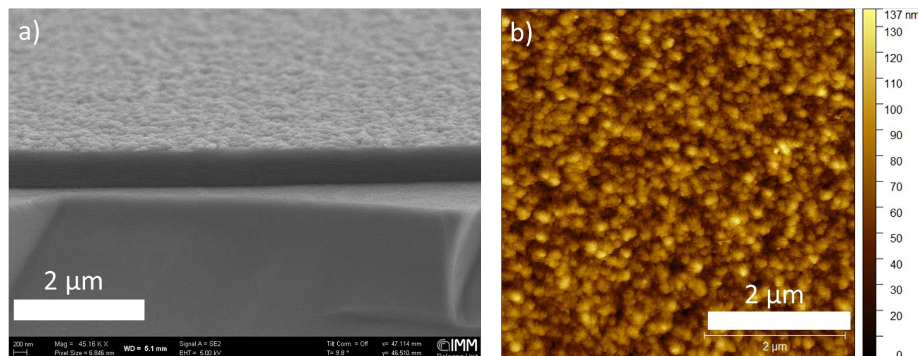


**Figure 1.** Cross section SEM micrograph of a C-cap on a 4H-SiC sample annealed at 1950 °C for 30 min (a) and AFM morphology of the C-cap surface (b).

Figs. 2(a-c) show the 1950 °C annealed 4H-SiC surface after dry oxidation. Two situations are identified in the SEM tilted cross section shown in Fig. 2(a): in the top region of the picture, i.e. the center of the sample, the surface is covered by clusters; in the lower region, i.e. close to the cleaved border, clusters are not detected. The low magnification image shown in Fig. 2(b) shows a location where the C-cap had been broken during cleavage before the oxidation, and confirms the coexistence of two different morphologies. The AFM micrograph in Fig. 2(c) is taken in the center of the sample. The surface is featured by the superposition of ripples 0.5-1 µm in size, and grains having 100-200 nm diameter.

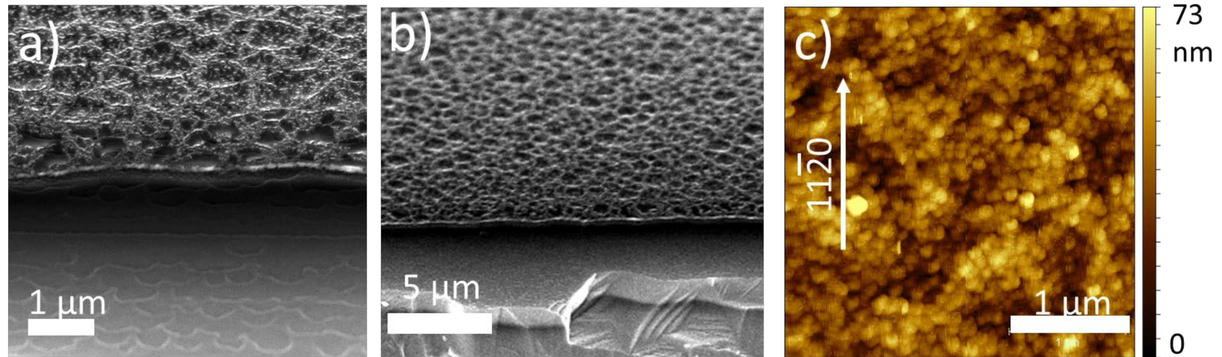


**Figure 2.** 4H-SiC surface after dry oxidation. High (a) and low (b) magnification SEM cross section views; AFM micrograph acquired in NCM (c).

In order to identify the composition of the clusters shown in Fig. 2(c), we analysed the evolution of the surface close to defects present on the as-implanted wafer, shown in Fig. 3(a). Though the rare occurrence of these defects is not detrimental for the process yield, their presence causes holes in the C-cap, which turned out to be useful for our analysis. Figs. 3(b) and 3(c) show SEM micrographs of the C-cap after 1950 °C 30 min annealing, and of the SiC surface after the C-cap removal, respectively. The sequence of Figs. 3(a-c) shows that the SiC surface not protected by the C-cap is eroded upon annealing, and that the incidence of clusters is reduced towards the center of the holes. Comparing the composition obtained from EDX microanalysis on regions with different cluster density allows to infer on the composition of the clusters. Fig. 3(d) shows an example EDX microanalysis. This picture is highly contrasted because the current for EDX measurements must be high in order to get a high number of counts. Indeed, the feature that we are analysing is located on the surface, while the composition is determined within a generation volume of about 600 nm diameter. For this reason, a high number of counts per analysed zone and a wide statistics are necessary to get reliable results. However, we noticed a repeatable difference in composition between regions with different cluster density.

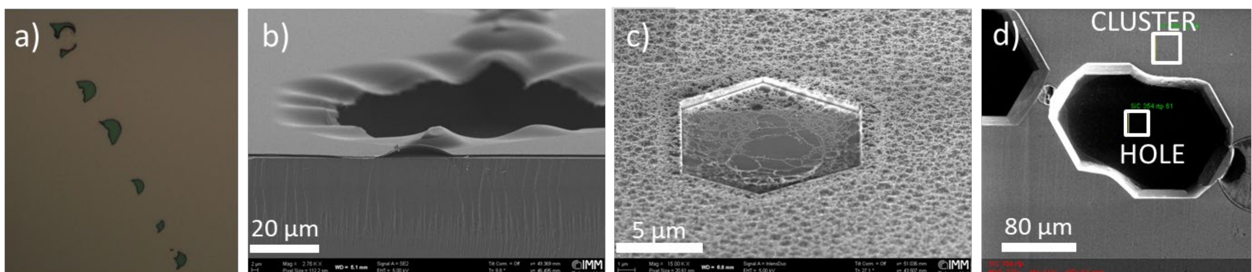


**Figure 3.** Optical micrograph of the defects on the $1\times 10^{19}$ $cm^{-3}$ Al as-implanted sample (a). Cross section SEM image of the C-cap in correspondence on one defect (b). Cross section SEM image of the SiC surface after C-cap removal (c); the location corresponding to a hole in the C-cap is etched off during the post-implantation annealing while a network of bright clusters covers the surface outside the etched hole. Plan view of an etched hole (d); the white rectangles show the regions where EDX was collected inside a hole (HOLE) and outside (CLUSTER).

Table 2 reports the C, Si and O atom concentration obtained by fitting of the EDX spectra in three locations on the 4H-SiC surface rich in clusters and four locations inside a hole, as shown in Fig. 3(d). EDX spectra were collected after C-cap removal. It is shown that the regions covered by the C-cap show slightly higher Si and O concentration with respect to the holes, where the C-cap was not present. Despite the limits of the technique, we can infer that the clusters observed on the surface can be made up of $SiO_2$.

**Table 2.** Location on the sample surface and compositional data obtained by EDX analyses: C, Si, and O atomic concentrations and Si to C ratio.

| CLUSTER/HOLE | C atom % | Si atom % | O atom % | Si/(Si+C) atom % |
|---|---|---|---|---|
| CLUSTER | 49.8 | 49 | 1.2 | 49.6 |
| CLUSTER | 49.9 | 48.9 | 1.2 | 49.5 |
| CLUSTER | 49.9 | 48.9 | 1.2 | 50.5 |
| HOLE | 51.5 | 47.7 | 0.7 | 48.1 |
| HOLE | 51.2 | 48.1 | 0.7 | 48.4 |
| HOLE | 51.3 | 48 | 0.7 | 48.3 |
| HOLE | 50.7 | 48 | 1.3 | 48.6 |

Figs. 4(a-f) show 5 × 5 µm2 AFM micrographs of the annealed C-cap in Figs. 4(a-c) and of the surfaces of 4H-SiC samples annealed in the very similar conditions after C-cap removal and BOE in Figs. 4(d-f). The arrow points the direction parallel to the major flat, i.e. <11-20>.

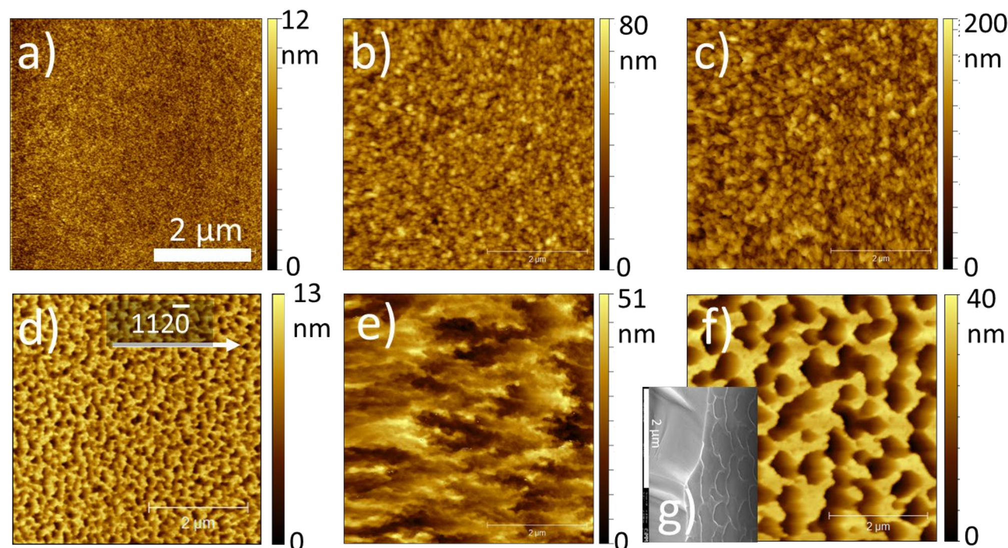


**Figure 4.** AFM micrographs of the annealed C-cap (a-c) and of the surfaces of 4H-SiC samples after C-cap removal and BOE (d-f). $1\times10^{20}$ cm$^{-3}$ Al implantation and annealing at 1700 °C for 15 min (a) and 30 min (d); $1\times10^{20}$ cm$^{-3}$ Al implantation and annealing at 1850 °C for 2 h (b,e); $1\times10^{19}$ cm$^{-3}$ Al implantation and annealing at 1950 °C for 30 min (c,f). The inset in (f) shows a cross section SEM micrograph of the border not covered by the C-cap during the removal, before BOE (g). The picture is rotated, the cleaved border is on the left.

Figs. 4(a,d) show the morphology of a C-cap on a $1\times10^{20}$ cm$^{-3}$ Al implanted sample annealed at 1700 °C for 15 min (Fig. 4(a)) and of the SiC surface of a sample annealed at 1700 °C for 30 min (Fig. 4(d)). Since the surface evolution at this temperature is slow [6], the image shown in Fig. 4(b) can be considered as representative of a 4H-SiC surface annealed for 15 min. Figs. 4 (b,e) show the morphologies of the C-cap (Fig. 4(b)), and of the corresponding $1\times10^{20}$ cm$^{-3}$ Al implanted 4H SiC (Fig. 4(e)), after annealing at 1850 °C for 2 h. Figs. 4 (c,f) show the morphology of the C-cap (Fig. 4(c)) and of the corresponding $1\times10^{19}$ cm$^{-3}$ Al implanted 4H-SiC surface (Fig. 4(f)) after annealing at 1950 °C for 30 min. These images show that surface roughening occurs both on the C-cap and on

the 4H-SiC surface but a one to one comparison shows no correspondence between the morphologies of the two surfaces with respect to ripple size and height. Fig. 4(g), represented as an inset of Fig. 4(f), shows a high magnification cross section SEM micrograph of the lower border of Fig. 2(a), i.e. the border of the sample that was not covered by the C-cap during the annealing in $O_2$, acquired before BOE. This picture, that represents a step backward with respect to the AFM micrograph in Fig. 4(f), is inserted to ease the comparison between the surface after BOE and the border before BOE. The remarkable similarity between the border shown in Figs. 2(a) and 4(g) and Fig. 4(f) suggests that a reaction occurring between the C-cap and the 4H-SiC during oxidation is unlikely.

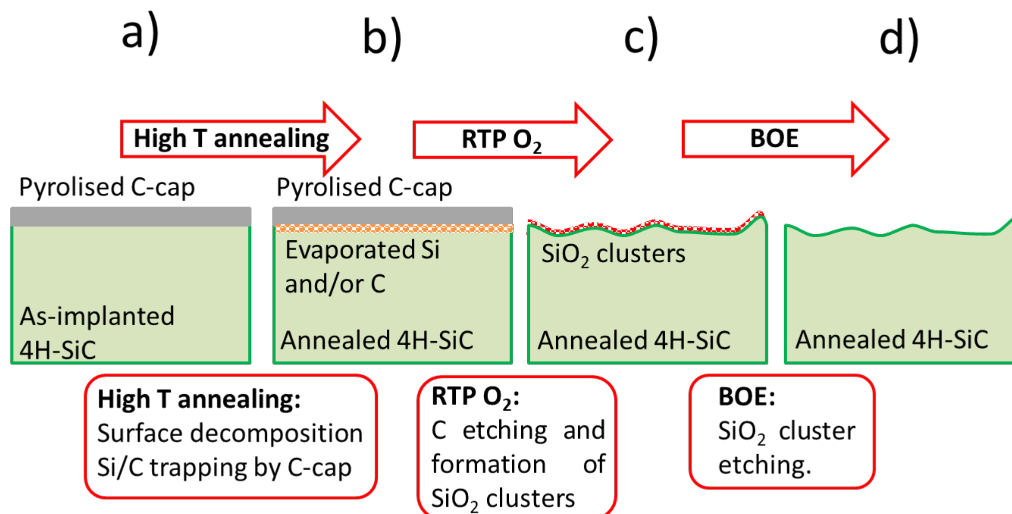


**Figure 5.** Schematic evolution of the C-cap and the SiC surface along the processing steps: before (a) and after (b)post-implantation annealing; after C-cap removal (c); after wet etching in BOE (d). The arrows between the panels represent the processing steps; the text boxes between the panels summarize the material evolution at each annealing step.

From our investigations it appears that the C-cap is not damaged during the annealing. Indeed, in order to perform this study, we focused on holes created in the C-cap by rare defects present on the wafer surface. Close to these defects, the surface evolves differently with respect to the rest of the wafer, where extensive analysis of the C-cap, and good process yield testified by electrical measurements [8], confirm that the greatest part of the C-cap is undamaged. Consequently, surface roughening due to C-cap deterioration is ruled out in our case. After the C-cap removal in dry $O_2$ the surface is covered by a network of clusters, probably made up $SiO_2$. The occurrence of such clusters only in regions which were covered by the C-cap during the oxidation allows to infer that the C-cap can trap Si or C atoms escaping from the SiC surface, and that the excess Si inside or under the C-cap is oxidized during the C-cap removal. Cross section transmission electron microscopy analyses are necessary to check the cluster composition, as well as to prove the occurrence and determine the location of Si trapping. However, independently on the effectiveness of the C-cap at trapping the atoms escaped from the surface, the surface roughness observed on Al-implanted 4H-SiC surfaces during high-temperature annealing is likely due to material evaporation.

Before the annealing, the pyrolysed C-cap is deposited on the SiC surface, Fig. 5(a). During the high temperature annealing the surface decomposes but the C-cap prevents the out-diffusion of Si and C atoms; at least a fraction of the escaped atoms remains trapped between the 4H-SiC surface and the C-cap surface. The occurrence depicted in Fig. 5(b) has not been detected. It could be verified for example by cross section TEM analyses. Though material evaporation is not proved here, this hypothesis is coherent with the conclusions drawn in reference [7], where material evaporation after high temperature annealing was detected by SIMS analyses. The dry oxidation, Fig. 5(c), removes the C-cap as well as the evaporated C atoms, while the evaporated Si or Si-C clusters oxidise; Si or Si-C clusters must be small enough to be completely oxidize in 15 min at 850 °C. It is not likely for

the SiC surface to oxidise because SiC oxidation takes place at much higher temperatures. The BOE wet etching removes the $SiO_2$ clusters completely, as it is represented in Fig. 5(d).

Despite the different methodology, the mechanism proposed in this paper is in agreement with the observations in reference [7]. However, with respect to reference [7], where the surface morphology after annealing is not characterized, we correlate the material erosion with surface roughening. We did not investigate any possible competition between material evaporation and the C atom supply by the C-cap during high temperature annealing [3]. In principle, the number of atoms involved in the surface rearrangement is far higher, and the two phenomena concern different regions of the samples, i.e. the surface and the epilayer, respectively. Figs. 5(a-d) summarize the mechanism proposed as an interpretation of our observations.

## Conclusions

This paper aims to shed light on the origin of the surface roughening observed in Al ion implanted 4H-SiC after high temperature annealing under a C-cap. Our analyses indicate that any C-cap deterioration during annealing and reactions taking place at the interface between the C-cap and the SiC during oxidation can be excluded. More likely, at temperatures as high as 1850 °C Si and C can evaporate from the surface, and get trapped inside or under the C-cap. While the excess C is removed in dry $O_2$, the excess Si oxidizes and is eventually removed in BOE solution.

## Acknowledgments

The technical staff of IMM Bologna is acknowledged for sample processing: Michele Bellettato, Fabrizio Tamarri and Michele Sanmartin.

## References

[1] R. Nipoti, A. Carnera, G. Alfieri, L. Kranz. About the Electrical Activation of $1\times10^{20}$ $cm^{-3}$ Ion Implanted Al in 4H-SiC at Annealing Temperatures in the Range 1500-1950 °C. Mat. Sci. Forum, 934 (2018) 333-338.

[2] H. M. Ayedh, V. Bobal, R. Nipoti, A. Hallén, B. G. Svensson. Formation of carbon vacancy in 4H silicon carbide during high-temperature processing. J. of Appl. Phys. 115 (2014) 012005.

[3] H. M. Ayedh, R. Nipoti, A. Hallén, B. G. Svensson. Elimination of carbon vacancies in 4H-SiC employing thermodynamic equilibrium conditions at moderate temperatures. Appl. Phys. Lett. 107 (2015) 252102.

[4] K. V. Vassilevski, N. G. Wright, I. P. Nikitina, A. B. Horsfall, A. G. O'Neill, M. J. Uren, K. P. Hilton, A. G. Masterton, A. J. Hydes, C. M. Johnson. Protection of selectively implanted and patterned silicon carbide surfaces with graphite capping layer during post-implantation annealing. Semicond. Sci. Technol. 20 (2005) 271-278.

[5] M. Spera, D. Corso, S. Di Franco, G. Greco, A. Severino, P. Fiorenza, F. Giannazzo, F. Roccaforte. Effect of high temperature annealing (T > 1650 °C) on the morphological and electrical properties of p-type implanted 4H-SiC layers. Materials Science in Semiconductor Processing 93 (2019) 274-279.

[6] M. Canino, P. Fedeli, C. Albonetti, R. Nipoti. 4H-SiC surface morphology after Al ion implantation and annealing with C-cap. J. of Microscopy 280 (2020) 229-240.

[7] M.K. Linnarsson, H.M. Ayedh, A. Hallén, L. Vines, B.G. Svensson. Surface erosion of ion-implanted 4H-SiC during annealing with carbon cap. Mat. Sci. Forum 924 (2018) 373-376.

[8] R. Nipoti, A. Parisini, V. Boldrini, S. Vantaggio, M. Canino, M. Sanmartin, G. Alfieri. $3\times 10^{18}$-$1\times10^{19}$ $cm^{-3}$ $Al^{+}$ ion implanted 4H-SiC: annealing time effect. Mat. Sci. Forum 1004 (2019) 683-688.